

Lobetyolin suppressed lung cancer in a mouse model by inhibiting epithelial-mesenchymal transition

Lu Liu, Zhankui Liu, Liu Yang, Xue Wu, Jiaying Zhu, Lili Liu, Yang Liu

Center for Clinical Drug Research and Development, The First Hospital of Qiqihar, Qiqihaer, Heilongjiang, China

ABSTRACT

Traditional Chinese medicines are gaining more attention as promising adjuvant agents for conventional chemotherapy. Recent studies have shown that lobetyolin (LBT) is one of the main bioactive compounds of traditional Chinese medicines and it exhibits anticancer activity in several types of cancer. Therefore, this study aimed to investigate the mechanism by which LBT inhibits lung cancer. A549 human lung cancer cells were treated with LBT. In addition, A549 cells were injected into Balb/c nude mice to establish model of lung cancer. The mice were treated with cisplatin (DDP) or LBT alone or in combination, and tumor growth was monitored. Protein levels of E-cadherin, vimentin and matrix metalloproteinase 9 (MMP9) were detected. We found that the combination of LBT and DDP showed stronger effect to inhibit the proliferation of A549 cells compared to LBT or DDP treatment alone. Wound healing assay showed that the ratio of wound healing was significantly lower in LBT group and DDP group and was the lowest in LBT+DDP group. Transwell invasion assay showed that the invasion ability of A549 cells was the weakest in LBT+DDP group. Protein levels of E-cadherin were the highest while those of vimentin and MMP9 were the lowest in A549 cells treated with LBT+DDP. Nude mouse xenograft tumor model showed that the combination of LBT with DDP had the highest efficacy to inhibit the growth of lung cancer, and tumor tissues of mice treated with LBT+DDP had the lowest expression of vimentin and MMP9 and the highest expression of E-cadherin. In conclusion, LBT significantly enhances the efficacy of chemotherapy on lung cancer, and the mechanism may be related to the inhibition of epithelial-mesenchymal transition.

Key words: Lobetyolin; lung cancer; cisplatin; epithelial-mesenchymal transition; Chinese traditional medicine.

Correspondence: Lu Liu, Center for Clinical Drug Research and development, The First Hospital of Qiqihar, 30 Gongyuan Road, Longsha District, Qiqihaer, Heilongjiang 161005, China. Tel. +86.0452.2549546.
E-mail: lil382st@gmail.com

Contributions: LL, designed the study; ZL, LY, XW, JZ, LL, YL performed experiments. All the authors read and approved the final version of the manuscript and agreed to be accountable for all aspects of the work.

Conflict of interest: The authors declare that they have no competing interests, and all authors confirm accuracy.

Ethics approval: The animal use protocol listed below has been reviewed and approved by the Animal Care and Use Committee of The First Hospital of Qiqihar, China (No. 072564).

Availability of data and materials: All data generated or analyzed during this study are included in this published article.

Introduction

Lung cancer is a leading cause of cancer related death and remains a big challenge for physicians.¹ Despite extensive investigations to develop novel anti-tumor drugs, cisplatin (DDP) is still a commonly used chemotherapy agent for non-small cell lung cancer (NSCLC). However, DDP has some adverse effects which impair the quality of life and even the survival of lung cancer patients.^{2,3} Therefore, traditional Chinese medicines are gaining more attention as promising adjuvant agents for conventional chemotherapy because they have shown noteworthy benefits in improving cancer patient survival and condition after cancer treatments.^{4,5}

Shenqi Fuzheng injection is a traditional Chinese medicine mainly consisted of two Chinese herbs *Radix codonopsis* and *Radix astragali*, and has demonstrated synergistic anti-tumor effect and reduced adverse effects during chemotherapy.^{6,7} Yangyin Fuzheng decoction (YYFZ) is a similar traditional Chinese compound medicine composed of 12 Chinese herbs, including *Radix codonopsis* and *Radix astragali*. Previous study reported that YYFZ enhanced the efficacy of DDP on lung cancer.⁸ However, the mechanism of anti-tumor action of YYFZ remains not fully understood. Recent studies have shown that lobetyolin (LBT) is one of the main bioactive compounds of traditional Chinese medicines such as Shenqi Fuzheng injection and YYFZ, and it exhibits anticancer activity in several types of cancer.^{9,10} In particular, LBT induced the apoptosis of colon cancer cells and lung cancer cells including A549 human lung cancer cells.¹¹⁻¹³

Epithelial-mesenchymal transition (EMT) indicates the process by which epithelial cells lose polarity and transform into mesenchymal cells. Under physiological conditions, EMT plays an important role in embryonic development and tissue repair. However, EMT is a driving force for the metastasis of malignant cancer.^{14,15} During EMT, the expression of epithelial markers such as E-cadherin is downregulated while the expression of mesenchymal markers such as vimentin is upregulated, leading to increased cancer cell migration and invasion. Matrix metalloproteinases (MMPs) are zinc-dependent endopeptidases that can degrade components of extracellular matrix (ECM) and induce EMT.¹⁶ In particular, MMP9 is a key protease for the degradation of ECM and promotes cancer development and metastasis.¹⁷ However, whether LBT could exert antitumor effects on lung cancer by inhibiting EMT remains unclear.

Therefore, in this study we aimed to investigate whether LBT enhances the efficacy of DDP on lung cancer *via* inhibiting EMT. We used A549 lung cancer cell line and nude mice implanted with A549 human lung cancer cell line as *in vitro* and *in vivo* models, and evaluated the effects of LBT alone or in combination with DDP on lung cancer cell growth, migration and invasion.

Materials and Methods

Cell culture

A549 human lung cancer cell line was purchased from American Type Culture Collection (Manassas, VA, USA) and cultured in DMEM medium supplemented with 10% fetal bovine serum (FBS) in a humid atmosphere at 37°C with 5% CO₂. LBT (purity >98%) was purchased from Absin Biotech (Shanghai, China), and DDP was purchased from Qilu Pharm (Jinan, China).

Cell proliferation assay

A549 cells were seeded in 96-well plates at the density of 2,000 cells/well, and then treated with PBS, 10 μM LBT, 5 μg/mL DDP, or the combination of 10 μM LBT and 5 μg/mL DDP. After treatment for 24, 48, 72 and 96 h, cell proliferation was examined by using Cell Counting kit-8 (KeyGen Biotech, Nanjing, China) with the absorbance at 450 nm measured by microplate reader.

Wound healing assay

A549 cells were seeded in 6-well plates at the density of 200,000 cells/well, and were grown to around 80% confluence. Next, a 20 μL pipette was used to gently scratch the cell monolayer. The plates were gently washed with PBS and culture medium was changed from complete DMEM medium to basic medium without FBS. The healing of the cell monolayer was examined under microscope at 0 and 24 h after the scratch.

Transwell invasion assay

A549 cells were seeded in chamber (Corning, NY, USA) pre-coated with matrigel at the density of 1×10⁴ cells/chamber. The top chamber was filled with DMEM medium, and the lower chamber was filled with 10% FBS. After incubation for 24 h, the membranes of the chamber were taken and the cells that have invaded into the membranes were stained with crystal violet and counted under microscope.

Western blot analysis

A549 cells were lysed in RIPA buffer. The lysates were centrifuged at 4°C, and the supernatants were collected to determine protein concentration by BSA method. The proteins were separated by 10% SDS-PAGE and transferred onto PVDF membranes (Millipore, Billerica, MA, USA). After blocking in 5% milk at room temperature for 1 h, the membranes were incubated with primary antibody for E-cadherin, vimentin, MMP9 or β-actin (Cell Signaling, Danvers, MA, USA) overnight at 4°C. The membranes were then washed and incubated with secondary antibody (Cell Signaling, Danvers, MA, USA) at room temperature for 1 h. The blots were developed with enhanced chemiluminescence kit (Pierce, Rockford, IL, USA), and the bands were quantified by using ImageJ software (Media Cybernetics, Rockville, MD, USA).

Animals

All animal experiments were approved by Animal Care and Use Committee of The First Hospital of Qiqihar (Qiqihar, China). BALB/c-nu/nu nude mice were provided by Qingdao Experimental Animal Center (Qingdao, China). A549 cells at log growth phase were collected and suspended at a concentration of 1 × 10⁷/mL PBS. 0.1 mL of suspension was injected into the right flank of mice. After 5 days, the diameter of the implanted xenografts reached 5 mm. The mice were divided randomly into 4 groups (n=6): control group intraperitoneally injected with equal amount of saline as in other groups once per day; LBT group intraperitoneally injected with LBT (10 mg/kg) once per day; DDP group intraperitoneally injected with DDP (2 mg/kg) once per three days; DPP+LBT group intraperitoneally injected with LBT (10 mg/kg) once per day and DDP (2 mg/kg) once per three days. The tumor growth was monitored by measuring tumor volume with the formula: tumor volume (mm³) = length (mm) × width (mm) × 0.5. At the end of experiments mice were euthanized by cervical dislocation to dissect tumor tissues.

Immunohistochemical staining

Tumor tissues were dissected from mice, fixed in 4% paraformaldehyde at 4°C overnight, and then embedded in paraffin

wax, and finally cut into 5 μm thick sections. The sections were incubated with 3% hydrogen peroxide for 30 min at room temperature to block endogenous peroxidase activity. After 30 min incubation with blocking serum, sections were incubated with antibody for E-cadherin, vimentin or MMP9 (all from Abcam, Cambridge, UK; 1:500 dilution in phosphate-buffered saline pH 7.2 containing 0.1% bovine serum albumin) overnight at 4°C. The sections were stained with DBA kit (ZSGB-Bio, Beijing, China) and counterstained with hematoxylin-eosin. The stained sections were observed under microscope and the intensity of staining was analyzed by using Image-J software. Staining intensity was scored according to a prespecified semiquantitative intensity scale: -, negative with no staining; +, weak staining intensity in >10% tumor cells; ++, moderate staining intensity in >10% tumor cells; +++, strong staining intensity in >10% tumor cells

Statistical analysis

All data were presented as mean \pm standard deviation (SD) and analyzed by using SPSS 18.0 software (SPSS Inc., Chicago, IL, USA). A p-value <0.05 was considered significant.

Results

LBT synergized with DDP to inhibit lung cancer cell proliferation and migration

Cell proliferation assay showed that LBT alone inhibited the proliferation of A549 cells in a time-dependent manner. Compared to LBT, DDP showed stronger effect to inhibit the proliferation of

A549 cells. However, the combination of LBT and DDP showed stronger effect to inhibit the proliferation of A549 cells (Figure 1A). Next, we performed wound healing assay and found that LBT inhibited wound healing of A549 cells at 24 h after the scratch. In comparison, DDP showed stronger ability to inhibit wound healing and the combination of LBT and DDP showed the strongest ability to inhibit wound healing (Figure 1B). Quantitative analysis showed that the ratio of wound healing was significantly lower in LBT group and DDP group than in PBS control group, and was the lowest in LBT+DDP group (Figure 1C). Taken together, these results showed that LBT synergized with DDP to inhibit lung cancer cell proliferation and migration.

LBT synergized with DDP to inhibit lung cancer cell invasion

Transwell invasion assay showed that LBT alone inhibited the invasion of A549 cells. Compared to LBT, the invasion ability of A549 cells was weaker in DDP group. Notably, the invasion ability of A549 cells was the weakest in LBT+DDP group (Figure 2A). To reveal the mechanism by which LBT synergized with DDP to inhibit lung cancer cell invasion, we examined the expression levels of EMT related proteins in A549 cells treated with PBS, LBT, DDP, LBT+DDP by Western blot analysis (Figure 2B). Densitometry analysis showed that protein levels of E-cadherin were significantly higher in LBT group and DDP group than in PBS group, and were the highest in LBT+DDP group. In contrast, protein levels of vimentin and MMP9 were significantly lower in LBT group and DDP group than in PBS group, and were the lowest in LBT+DDP group (Figure 2C). Collectively, these results indicated that LBT synergized with DDP to inhibit EMT and invasion of lung cancer cell.

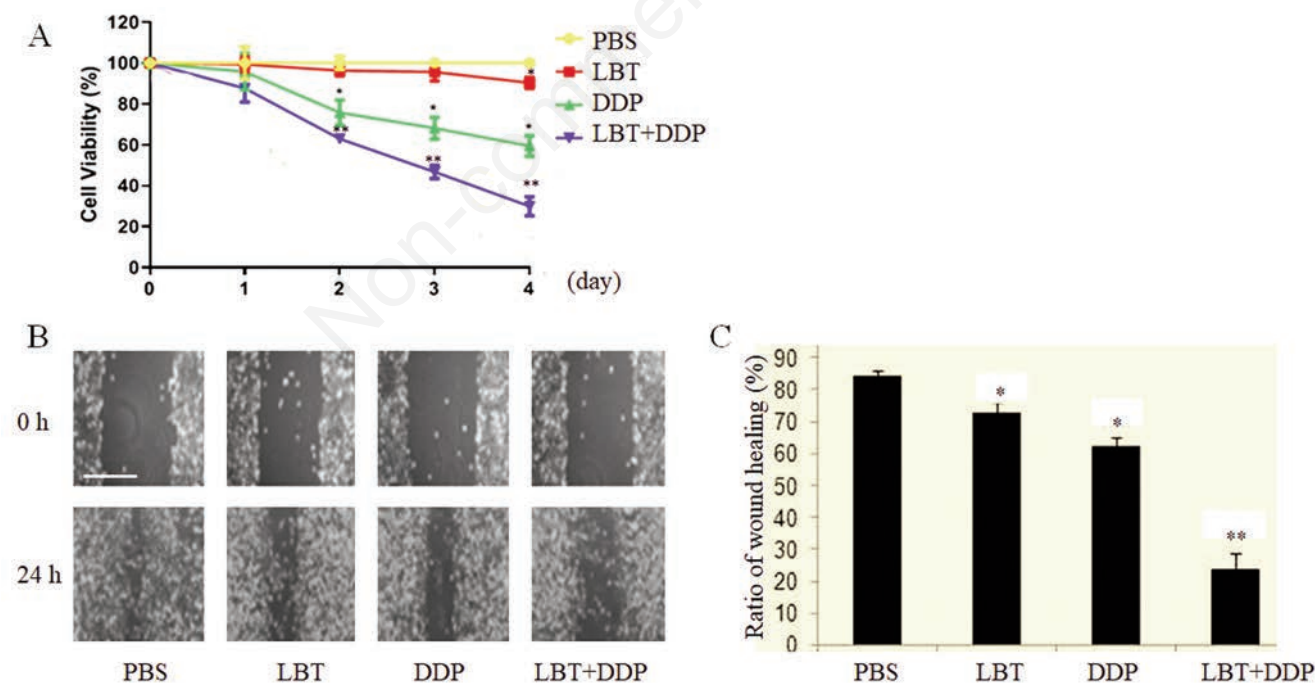


Figure 1. LBT synergized with DDP to inhibit lung cancer cell proliferation and migration. A) CCK-8 assay of the viability of A549 cells after treatment with PBS, 10 μM LBT, 5 $\mu\text{g}/\text{mL}$ DDP, or the combination of 10 μM LBT and 5 $\mu\text{g}/\text{mL}$ DDP up to 4 days. B) Wound healing assay of the migration ability of A549 cells after treatment with PBS, 10 μM LBT, 5 $\mu\text{g}/\text{mL}$ DDP, or the combination of 10 μM LBT and 5 $\mu\text{g}/\text{mL}$ DDP at 0 h and 24 h after scratch; scale bar: 10 mm. C) Quantitative analysis of the results of wound healing assay; * p <0.05, ** p <0.01 vs PBS group (n=6).

LBT synergized with DDP to inhibit tumor cancer growth and EMT in nude mice

Next, we established nude mice xenografted with A549 lung cancer cells as an *in vivo* model to confirm anti-tumor effect of LBT. Tumor growth curve showed that the combination of LBT with DDP had the highest efficacy to inhibit the growth of lung cancer (Figure 3A). At the end of experiments, we dissected tumor tissues from nude mice and found that tumor size was the smallest in group treated with the combination of LBT and DDP (Figure

3B). By immunohistochemical analysis we found that the expression of vimentin and MMP9 was lower while the expression of E-cadherin was higher in each treatment group compared to PBS group (Figure 4A). Quantitative analysis of the staining of E-cadherin, vimentin and MMP9 showed that combination treatment group had the lowest expression levels of vimentin and MMP9 and the highest expression levels of E-cadherin (Figure 4B). These results suggested that LBT synergized with DDP to inhibit EMT of lung cancer *in vivo*.

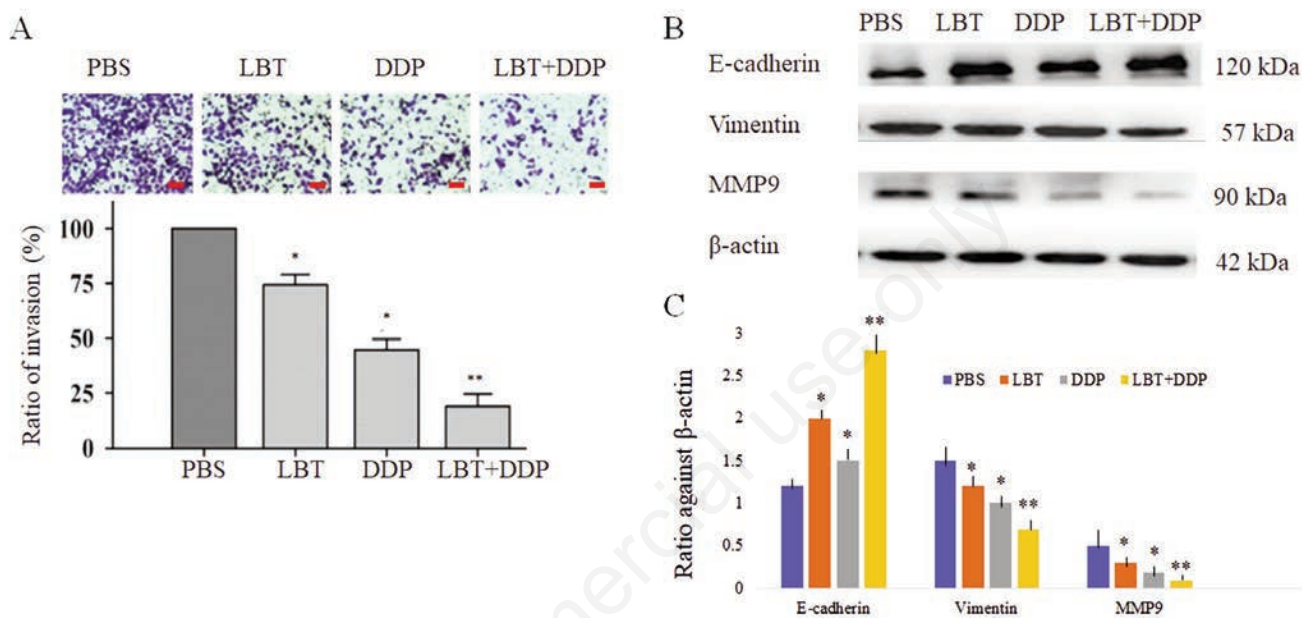


Figure 2. LBT synergized with DDP to inhibit lung cancer cell invasion. A) Transwell invasion assay of the invasion ability of A549 cells after treatment with PBS, 10 μ M LBT, 5 μ g/mL DDP, or the combination of 10 μ M LBT and 5 μ g/mL DDP; scale bar: 5 μ m. B) Western blot analysis of E-cadherin, vimentin and MMP9 in A549 cells after treatment with PBS, 10 μ M LBT, 5 μ g/mL DDP, or the combination of 10 μ M LBT and 5 μ g/mL DDP; β -actin was loading control. C) Densitometry analysis of relative protein levels of E-cadherin, vimentin and MMP9 in A549 cells after treatment with PBS, 10 μ M LBT, 5 μ g/mL DDP, or the combination of 10 μ M LBT and 5 μ g/mL DDP; * p <0.05, ** p <0.01 *vs* PBS group ($n=3$).

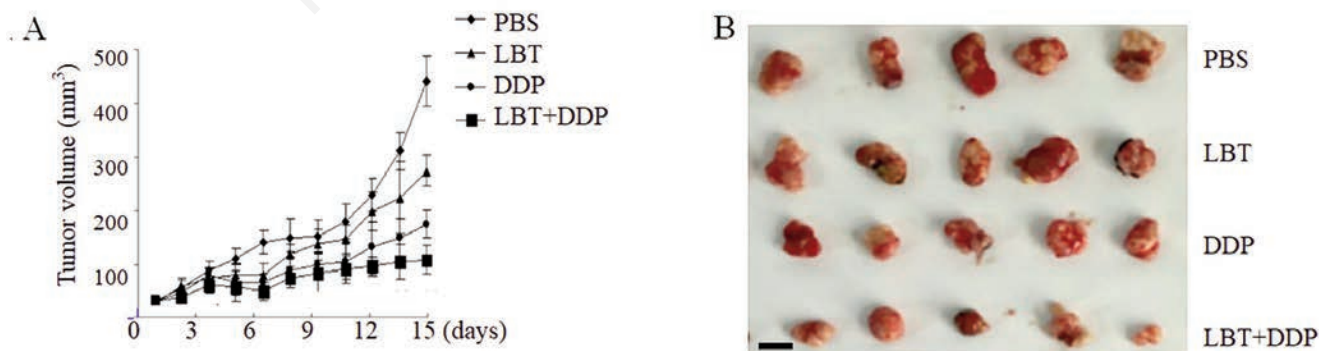


Figure 3. LBT enhanced anti-tumor efficacy of DDP on lung cancer in nude mice. A) The growth of tumor xenografted from A549 cells in nude mice was monitored by measurement of tumor volume up to 15 days after treatment with PBS once per day (PBS group), LBT (10 mg/kg) once per day (LBT group), DDP (2 mg/kg) once per three days (DDP group), LBT (10 mg/kg) once per day and DDP (2 mg/kg) once per three days (DDP+LBT group). B) The tumor tissues dissected from each mouse in different groups (PBS, LBT, DDP, LBT+DDP) ($n=5$) at the end of experiments; scale bar: 5 mm.

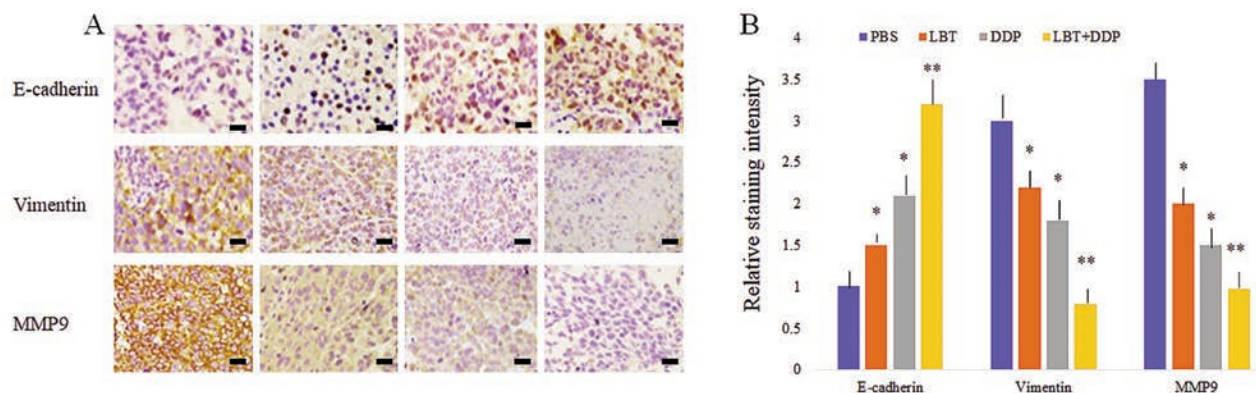


Figure 4. The effects of LBT on EMT markers in lung cancer xenograft in nude mice. A) Immunohistochemical staining of E-cadherin, vimentin and MMP9 in tumor tissues dissected from nude mice; scale bar: 50 μ m. B) Quantitative analysis of relative staining intensity; * $p < 0.05$, ** $p < 0.01$ vs PBS group (n=3).

Discussion

In this study, we first examined the anti-tumor efficacy of LBT, a main component of traditional Chinese medicine YYFZ, on lung cancer cell proliferation, migration and invasion *in vitro*. Next, we confirmed the anti-tumor efficacy of LBT in nude mouse model of lung cancer xenograft. Both *in vitro* and *in vivo* data revealed that LBT could synergize with DDP to inhibit EMT of lung cancer.

YYFZ is composed of 12 Chinese medicinal herbs including *Radix codonopsis*, *Radix astragali*, *Radix glehniae*, *Gigeria galli*, *Glycyrrhizae*, *Herba hedyotidis diffusae*, *Radix ophiopogonis*, *Pericarpium citri reticulatae*, *Radix angelicae sinensis*, *Poria*, *Rhizoma dioscoreae*, and *Radix asparagi*, which have been shown to enhance the efficacy of radiotherapy or chemotherapy on advanced oesophageal cancer.¹⁸ Previously, traditional Chinese medicine YYFZ was shown to enhance the efficacy of DDP on lung cancer, but the underlying mechanism is elusive. Previous study reported that another traditional Chinese medicine Bu-Fei decoction inhibited lung cancer by attenuating EMT of lung cancer cells, and LBT is one important component of Bu-Fei decoction.¹⁹ Therefore, in this study we focused on LBT as one main component of YYFZ, and found that LBT inhibited the proliferation, migration and invasion of lung cancer cells by inhibiting EMT. Interestingly, a recent study reported that traditional Chinese medicine Jian-pi-yang-zheng (mJPYZ) decoction could inhibit the proliferation, migration and invasion of gastric cancer cells by inhibiting EMT, and LBT was identified as one of the main components of mJPYZ.²⁰ These results suggest that a variety of traditional Chinese medicine may exert anti-tumor efficacy by inhibiting EMT of cancer cells.

DDP is a first-line chemotherapy drug for lung cancer, but it has side effects and the treatment efficacy varies depending on the conditions of lung cancer patients.^{21,22} Therefore, there is an urgent need to develop combination therapy to improve the efficacy and reduce the toxicity of DDP. In this study, we investigated the synergistic effects of LBT and DDP on lung cancer therapy. *In vitro* results demonstrated that the combination of LBT and DDP exerted significantly higher efficacy in the inhibition of lung cancer cell proliferation, migration and invasion, accompanied by higher expression of E-cadherin and lower expression of vimentin and MMP9, compared to LBT or DDP treatment alone. Furthermore, *in vivo* results showed that the combination of LBT and DDP significantly inhibited the growth of xenografted lung cancer in nude

mouse model compared to LBT or DDP treatment alone. More importantly, the combination of LBT and DDP upregulated E-cadherin expression and downregulated vimentin and MMP9 expression in xenografted cancer tissues, confirming that LBT enhances chemotherapy efficacy of DDP on lung cancer by inhibiting EMT.

Previous study showed that Bu-Fei decoction attenuated EMT of lung cancer *via* the inhibition of transforming growth factor β 1 signaling pathway.¹⁹ Recent study suggested that LBT may inhibit EMT of gastric cancer *via* the regulation of glycolysis pathway.²⁰ Indeed, glycolysis was associated with the apoptosis and DDP resistance of lung cancer cells.²³ Moreover, Akt/mTOR signaling regulated proliferation, migration, and glycolysis of lung cancer cells.²⁴ Therefore, further studies are needed to investigate whether LBT regulates Akt/mTOR signaling and glycolysis pathway to inhibit EMT of lung cancer.

In conclusion, our results suggest that LBT enhances chemotherapy efficacy on lung cancer by inhibiting EMT. Further studies are needed to verify whether LBT could be used as an adjunct agent for lung cancer chemotherapy.

References

- Wang J, Wang Y, Tong M, Pan H, Li D. Research progress of the clinicopathologic features of lung adenocarcinoma. *Onco Targets Ther* 2018;11:7011-7.
- Zhang D, Tong LX, Wang QJ, Cao YF, Gao Y, Yang DH, et al. Diagnosis of lung cancer based on plasma metabolomics combined with serum markers. *Oncologie* 2020;22:75-82.
- Dempke WC. Targeted therapy for NSCLC -- A double-edged sword? *Anticancer Res* 2015;35:2503-12.
- Hadda T B, Kamaruddin M, Patel S. Reversal of multidrug resistance and antitumor promoting activity of 3-oxo-6 β -hydroxy- β -amyrin isolated from *Pistacia integerrima*. *Biocell* 2021;45:139-47.
- Cao C, Han D, Su Y, Ge Y, Chen H, Xu A. Ginkgo biloba exocarp extracts induces autophagy in Lewis lung cancer cells involving AMPK / mTOR / p70S6k signaling pathway. *Biomed Pharmacother* 2017;93:1128-35.
- Cao DD, Xu HL, He AB, Xu XM, Ge W. The effect of ShenQi FuZheng injection in combination with chemotherapy versus chemotherapy alone on the improvement of efficacy and immune function in patients with advanced non-small cell lung

- cancer: A meta-analysis. *PLoS One* 2016;11:e0152270.
7. Xu R, Lin L, Li Y, Li Y. ShenQi FuZheng Injection combined with chemotherapy in the treatment of colorectal cancer: A meta-analysis. *PLoS One* 2017;12:e0185254.
 8. Wei D, Wang L, Chen Y, Yin G, Jiang M, Liu R, et al. Yangyin Fuzheng Decoction enhances anti-tumor efficacy of cisplatin on lung cancer. *J Cancer* 2018;9:1568-74.
 9. Bailly C. Anticancer properties of lobetyolin, an essential component of *Radix Codonopsis* (Dangshen) *Nat Prod Bioprospect* 2021;11:143-53.
 10. Wang J, Tong X, Li P, Cao H, Su W. Immuno-enhancement effects of Shenqi Fuzheng injection on cyclophosphamide-induced immunosuppression in Balb/c mice. *J Ethnopharmacol* 2012;139:788-95.
 11. He W, Tao W, Zhang F, Jie Q, He Y, Zhu W, et al. Lobetyolin induces apoptosis of colon cancer cells by inhibiting glutamine metabolism. *J Cell Mol Med* 2020;24:3359-69.
 12. Wang MC, Wu YF, Yu WY, Yu B, Ying HZ. Polyacetylenes from *Codonopsis lanceolata* root induced apoptosis of human lung adenocarcinoma cells and improved lung dysbiosis. *Biomed Res Int* 2022;2022:7713355.
 13. Phan NHT, Thuan NTD, Hien NTT, Huyen PV, Duyen NHH, Hanh TTH, et al. Polyacetylene and phenolic constituents from the roots of *Codonopsis javanica*. *Nat Prod Res* 2022;36:2314-20.
 14. Hanahan D, Weinberg RA. Hallmarks of cancer: the next generation. *Cell* 2011;144:646-74.
 15. Chen X, Zhang H, Li L, Chen W, Bao T, Li B. miR-5100 mediates migration and invasion of melanomatous cells in vitro via targeting SPINK5. *J Compr Mol Sci Genet* 2021;1:14-23.
 16. Cao L, Yang DM, Bai B. Mir-1247 affects the proliferation, invasion and apoptosis of osteosarcoma cells through SOX9. *Oncologie* 2021;23:149-58.
 17. Bassiouni W, Ali MAM, Schulz R. Multifunctional intracellular matrix metalloproteinases: implications in disease. *FEBS J* 2021;288:7162-82.
 18. Chen X, Deng L, Jiang X, Wu T. Chinese herbal medicine for oesophageal cancer. *Cochrane Database Syst Rev* 2016;(1):CD004520.
 19. He XR, Han SY, Li XH, Zheng WX, Pang LN, Jiang ST, et al. Chinese medicine Bu-Fei decoction attenuates epithelial-mesenchymal transition of non-small cell lung cancer via inhibition of transforming growth factor β 1 signaling pathway in vitro and in vivo. *J Ethnopharmacol* 2017;204:45-57.
 20. Sun Q, Yuan M, Wang H, Zhang X, Zhang R, Wang H, et al. PKM2 is the target of a multi-herb-combined decoction during the inhibition of gastric cancer progression. *Front Oncol* 2021;11:767116.
 21. Yang G, Hao X, Hu J, Dong K, Xu H, Yang L, et al. Pyrotinib in HER2 heterogeneously mutated or amplified advanced non-small cell lung cancer patients: a retrospective real-world study (PEARL). *J Natl Cancer Cent* 2021;1:139.
 22. Zhong J, Li X, Wang Z, Duan J, Li W, Zhuo M, et al. Evolution and genotypic characteristics of small cell lung cancer transformation in non-small cell lung carcinomas. *J Natl Cancer Cent* 2021;1:153.
 23. Zhang S, Lv X, Li L, Luo Y, Xiang H, Wang L, et al. Melittin inhibited glycolysis and induced cell apoptosis in cisplatin-resistant lung adenocarcinoma cells via TRIM8. *Biocell* 2021;45:167-75.
 24. Gu F, Zhang J, Yan L, Li D. CircHIPK3/miR-381-3p axis modulates proliferation, migration, and glycolysis of lung cancer cells by regulating the AKT/mTOR signaling pathway. *Open Life Sci* 2020;15:683-95.

Received for publication: 19 April 2022. Accepted for publication: 24 June 2022.

This work is licensed under a Creative Commons Attribution-NonCommercial 4.0 International License (CC BY-NC 4.0).

©Copyright: the Author(s), 2022

Licensee PAGEPress, Italy

European Journal of Histochemistry 2022; 66:3423

doi:10.4081/ejh.2022.3423

Publisher's note: All claims expressed in this article are solely those of the authors and do not necessarily represent those of their affiliated organizations, or those of the publisher, the editors and the reviewers. Any product that may be evaluated in this article or claim that may be made by its manufacturer is not guaranteed or endorsed by the publisher.